Supporting Online Material

Materials and Methods

Planktonic foraminiferal $\delta^{18}O$ and Mg/Ca

Core MD97-2120 was sampled at 2 cm intervals for stable oxygen isotope analyses on *Globigerina bulloides* (250-355 µm). Twenty-five specimens of each sample were cleaned following standard laboratory protocols (*S1*) and analyzed on a Thermo-Finnigan MAT 252 mass spectrometer with automated Carbo Kiel III carbonate preparation device. A benthic $\delta^{18}O$ section was measured from 530-1095 cm core depth on mono-specific samples of *Cibicidoides wuellerstorfi, C. cicatricosus* and *C. kullenbergi,* and complemented by analyses on *Melonis barleeanum* in core intervals lacking *Cibicidoides* spp. specimens. To all benthic $\delta^{18}O$ values 0.64‰ were added to correct for the species-specific isotope fractionation. Precision for $\delta^{18}O$ was 0.02‰ over the period of analyses as checked by routine runs of NBS19. All isotope values are reported on the VPDB scale. Mg/Ca analyses on *G. bulloides* (250-315 µm) were run on a subset of samples with 10 cm spacing. Twenty specimens per sample were cleaned in successive steps following the cleaning protocol of Barker *et al.* (*S2*) and analyzed on a Varian Vista ICP-AES using an intensity ratio calibration (*S3*). Accuracy (precision), as checked by routine measurements of a quality standard, varied between 0.01% and 0.9% (0.1-0.5%) over the two month period the analyses were carried out, with an average accuracy (precision) of 0.2% (0.3%) over this period. Precision of ten replicate analyses of foraminiferal samples was ±5.8% (1σ) for Mg/Ca equivalent to ±0.5°C in SST at 11.6ºC.

Sea surface temperature (SST) estimates

We used the Mg/Ca-SST calibration of Mashiotta *et al.* (*S4*), that is based on cultured *G. bulloides* and two core-top values from the Subantarctic Southern Ocean: $Mg/Ca = 0.474\exp(0.107T)$, with Mg/Ca in mmol/mol and T representing SST in degrees Celsius. This is equivalent to the calibration by Elderfield and Ganssen (*S5*) which yields temperatures at subsurface foraminiferal calcification habitats, whereas that by Mashiotta *et al.* (*S4*) is tuned to sea surface temperatures. The estimated temperature offset between the two different calibrations is 0.9 ±0.1ºC for our data, which is close to the 1ºC offset

between summer SST and the temperature at the depth habitat of *G. bulloides* suggested by Duplessy *et al.* (*S6*).

Age control 0-35 ka - ^{14}C AMS dates

Radiocarbon dating on planktonic foraminifera was carried out at the Leibniz-Laboratory for Radiometric Dating and Isotope Research of the University of Kiel, Germany. We calibrated all ^{14}C ages younger than 20 ka with the Calib4.3 program (*S7*) using the marine calibration data set INTCAL98 (0-24 cal. ka) (*S8*). The three ages between 26.6 and 32.3 ^{14}C ka were calibrated using a Northern Hemisphere marine data set (*S9*) of ^{14}C *vs*. calendar year age offset that follows the evolution of geomagnetic paleointensity (*S10*). A local ^{14}C reservoir age correction of 240 ±40 a (*S11*) yields results that are in good agreement with ages that would result from provisionally tuning the benthic δ^{18}O record of core MD97-2120 to that of Northeast Atlantic core MD95-2042 (*S12*), which is tied to the Greenland GISP2 chronology. Discrepancies between the calibrated radiocarbon ages and the benthic δ^{18}O-tuned age-scale between 30-36 ka of up to 630 years are within the uncertainty (±450 to ±650 a) of the marine-controlled data set (*S9*). Taking the age differences between radiocarbon and tuned ages at face value suggests local reservoir ages for this period of 677-1,270 years, approaching the reservoir age of 1,970 years that has been estimated from paired Kawakawa ash and marine sediment radiocarbon dating (*S11*).

We discarded two ^{14}C dates (16.38, 16.67 ka, equivalent to 18.68, 19.01 cal. ka) that deviate considerably from the otherwise strongly linear age *vs*. core-depth correlation (Fig. S1). Using both these ages in age modeling causes the planktonic δ^{18}O record in the section 300-447 cm to be compressed and the section 447-525 cm to be expanded. This goes along with a transient swing of sedimentation rates from 3.5 cm/ka to >170 cm/ka (whole core-mean is 16 cm/ka), which we consider implausible given the linear age-depth relation that exists for the radiocarbon dated section. Both dates were generated from small carbonate samples (Table S1) further causing concern regarding their reliability. Two age reversals occur in the sequence of AMS datings, one at 168-193 cm and another one at 266-303 cm. In both cases we applied ages from the linear age *vs*. depth relation (Table S1, Fig. S1).

Table S1: ^{14}C AMS ages analyzed on planktonic foraminifera and calibrated ages for core MD97-2120

Lab code	Depth (cm)	Species	Foram tests	mg C	Conventional ^{14}C age (yr)	± 1s (yr)	Calibrated ^{14}C age (yr)	± 1s (yr)	
KIA 18807	22-23	*G. b.*	800	1.1	2,585	± 30	1,951*	+ 58/- 56	
KIA 18808	36-37	*G. b.*	900	1.3	3,895	± 60	3,557*	+ 80/- 96	
KIA 18809	98-99	*G. b.*	940	1.2	7,560	± 40	7,764*	+ 65/- 63	
KIA 18810	168-169	*G. b.*	850	0.9	10,550	± 50	10,941*	+ 226/- 61	§
KIA 18811	192-193	*G. b.*	920	1	10,650	± 55	10,917*	+ 421/- 12	§
KIA 18812	202-203	*G. b.*	1100	1.1	11,240	± 50	12,472*	+ 151/- 80	
KIA 18813	230-231	*G. b.*	910	0.8	12,665	± 60	13,942*	+ 89/- 94	
KIA 18814	252-253	*G. b.*	1450	1.2	13,155	± 60	14,345*	+ 940/- 162	
KIA 18815	266-267	*G. b.*	850	1.2	14,730	± 70	16,778*	+ 256/- 245	‖
KIA 18816/17	300-303	*G. b.+ N. p.*	749	0.5	14,040	± 80	15,984*	+ 245/- 240	‖
KIA 18821	390-392	*G. b.+ N. p.*	854	0.08	16,380	± 190	18,677*	+ 372/- 353	‡
KIA 18823	446-447	*G. b.+ N. p.*	631	0.6	16,670	± 100	19,010*	+ 328/- 311	‡
KIA 18824	524.5-525.5	*G. b.+ N. p.*	942	1.1	26,610	± 220	29,570†	± 700	
KIA 18825	572.5-573.5	*G. b.+ N. p.*	803	0.6	29,650	+ 320/- 310	33,010†	± 700	
KIA 18826	632.5-633.5	*G. b.+ N. p.*	823	1	32,300	+ 430/- 410	35,260†	± 800	

G.b.: Globigerina bulloides, N.p.: Neogloboquadrina pachyderma.

* calibrated using the Calib4.3 computer program of Stuiver and Reimer (*S7*).

† calibrated using the data set of Voelker *et al.* (*S9*).

‡ discarded dates.

§ both ages are identical within the error bars, an interpolated mean age of 11.11 cal. ka was applied (see also Fig. S1).

‖ age reversal, interpolated mean age of 16.7 cal. ka was applied (see also Fig. S1).

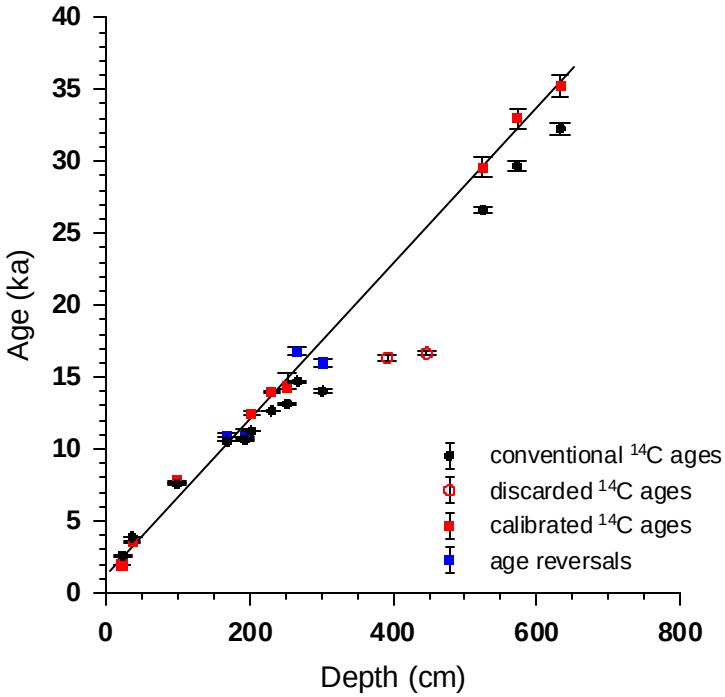

Fig. S1: ^{14}C AMS ages for core MD97-2120. Uncorrected radiocarbon ages (black dots) and calibrated ages (red squares) plotted against depth in core. Discarded dates are shown as open red circles. Blue squares are age reversals for which interpolated ages were computed applying the linear age *vs*. depth regression through all calibrated ages except for the two rejected ages (y = 0.054x + 1.365). The mean of two interpolated ages was then used for the age model of MD97-2120.

Age control >35 ka – graphic correlation

For age control in the time interval 40-72 ka a benthic δ^{18}O section from core MD97-2120 was graphically fitted to a similar section from Northeast Atlantic core MD95-2042 (37º47.99'N, 10º09.99'W, 3146 m) (*S12*) (Fig. S2; see main text for discussion).

The age scale for the time interval 72-341 ka was developed by graphical correlation of our SST record with the Vostok δD record (*S13*) on its orbitally tuned age scale (*S14*). A complete listing of age control points used to derive the age model for core MD97-2120 is given in Table S2.

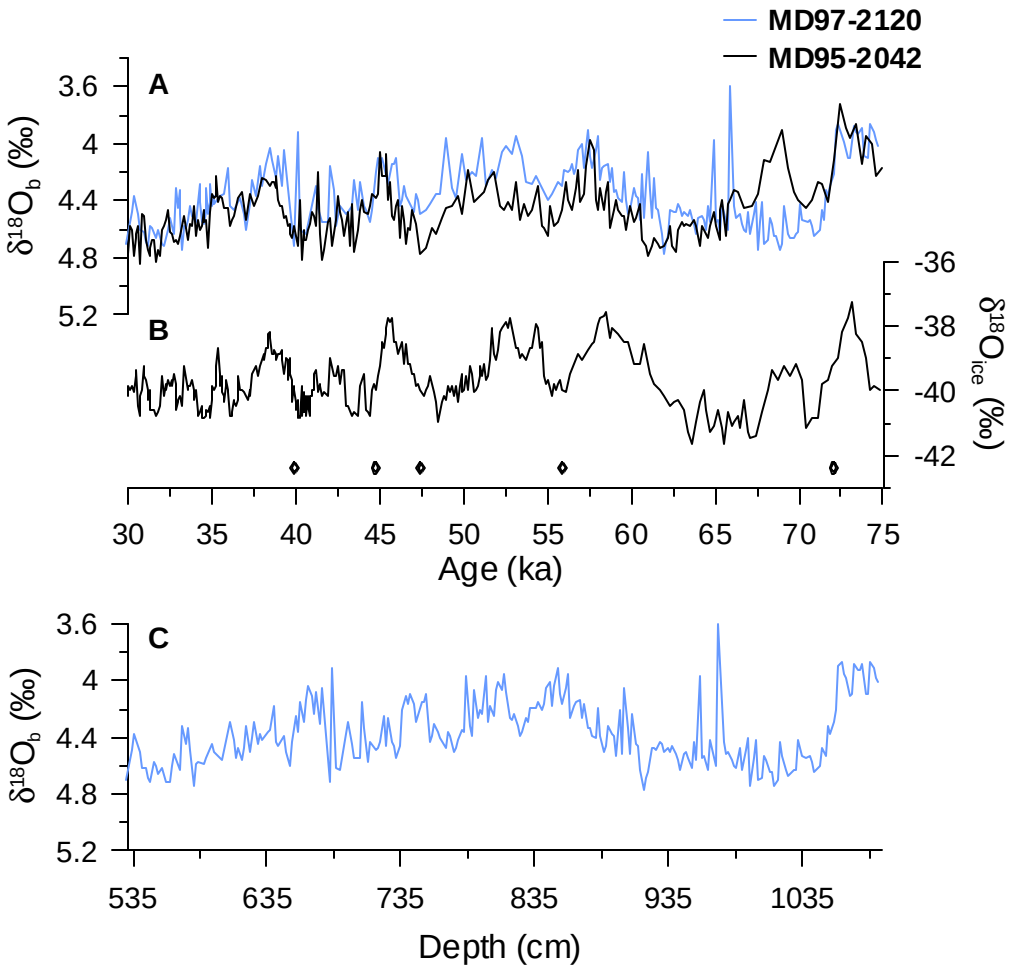

Fig. S2: Correlation of last glacial benthic $\delta^{18}O$ sections of core MD97-2120 and Northeast Atlantic core MD95-2042 (*S12*). The Antarctic Byrd $\delta^{18}O_{ice}$ record is shown for comparison. (**A**) Benthic $\delta^{18}O$ records of Southwest Pacific core MD97-2120 (45º32.06'S, 174º55.85'E) (blue) and Northeast Atlantic core MD95-2042 (37º47.99'N, 10º09.99'W) (black) versus age. (**B**) $\delta^{18}O_{ice}$ record of Antarctic Byrd ice core versus age (*S15*). (**C**) Benthic $\delta^{18}O$ section of core MD97-2120 plotted along depth in core. Diamonds indicate age tie-points used to align the benthic $\delta^{18}O$ sections.

Table S2: Age control points for core MD97-2120

Depth (cm)	Age (ka)	Age control points	^{14}C calibration & references
22.5	1.95	^{14}C AMS	Calib4.3 (*S7*)
36.5	3.56	^{14}C AMS	Calib4.3 (*S7*)
98.5	7.76	^{14}C AMS	Calib4.3 (*S7*)
180.5	11.11	^{14}C AMS reversal, interpolated	Calib4.3 (*S7*)
202.5	12.47	^{14}C AMS	Calib4.3 (*S7*)
230.5	13.94	^{14}C AMS	Calib4.3 (*S7*)
252.5	14.35	^{14}C AMS	Calib4.3 (*S7*)
284	16.70	^{14}C AMS reversal, interpolated	Calib4.3 (*S7*)
471	26.17	Kawakawa tephra	(*S16*, *S17*)
525	29.57	^{14}C AMS	(*S9*)
573	33.01	^{14}C AMS	(*S9*)
633	35.26	^{14}C AMS	(*S9*)
683.25	40.02	$\delta^{18}O_b$ tuned to $\delta^{18}O_b$ of MD95-2042	(*S12*)
737.25	44.83	$\delta^{18}O_b$ tuned to $\delta^{18}O_b$ of MD95-2042	(*S12*)
775.25	47.54	$\delta^{18}O_b$ tuned to $\delta^{18}O_b$ of MD95-2042	(*S12*)
831.25	55.98	$\delta^{18}O_b$ tuned to $\delta^{18}O_b$ of MD95-2042	(*S12*)
1061.25	72.13	$\delta^{18}O_b$ tuned to $\delta^{18}O_b$ of MD95-2042	(*S12*)
1451.25	105.14	SST tuned to Vostok δD	Vostok age model of (*S14*)
1651.25	135.28	SST tuned to Vostok δD	Vostok age model of (*S14*)
1991.25	161.06	SST tuned to Vostok δD	Vostok age model of (*S14*)
2071.25	168.71	SST tuned to Vostok δD	Vostok age model of (*S14*)
2241.25	180.91	SST tuned to Vostok δD	Vostok age model of (*S14*)
2491.25	220.32	SST tuned to Vostok δD	Vostok age model of (*S14*)
2561.25	233.34	SST tuned to Vostok δD	Vostok age model of (*S14*)
2741.25	245.55	SST tuned to Vostok δD	Vostok age model of (*S14*)
2911.25	262.59	SST tuned to Vostok δD	Vostok age model of (*S14*)
3211.25	281.73	SST tuned to Vostok δD	Vostok age model of (*S14*)
3351.25	298.83	SST tuned to Vostok δD	Vostok age model of (*S14*)
3491.25	315.92	SST tuned to Vostok δD	Vostok age model of (*S14*)
3621.25	337.80	SST tuned to Vostok δD	Vostok age model of (*S14*)

Sea surface salinity (SSS) estimates

We used the mean-ocean $\delta^{18}O_w$ record of Waelbroeck *et al.* (*S18*) to eliminate the global ice volume signal from the planktonic $\delta^{18}O_{plk}$ record: $\delta^{18}O_{plk}$ - $\delta^{18}O_w$. Prior to subtraction, the records were aligned in their chronologies to minimize artifacts arising from temporal offsets. Next we sampled the ice volume corrected $\delta^{18}O_{plk}$ record, $\delta^{18}O_c$, at the timestep of the lower resolution $SST_{Mg/Ca}$ record and used both data series as input into the low-temperature paleotemperature equation of Shackleton (*S19*) to extract seawater $\delta^{18}O_w$: $T = 16.9 - 4.0(\delta^{18}O_c - \delta^{18}O_w)$. $\delta^{18}O_w$ was then converted into a local salinity record by using a $\delta^{18}O_w$-salinity relation based on surface ocean data from latitudes 40º-50ºS compiled by

Schmidt et al. (*S20*): $S = 1.465\ \delta^{18}O_w + 34.00$; $r^2 = 0.81$. The salinity change arising from millennial-scale sea level fluctuations of 10-15 m (*S21*) not resolved in the mean-ocean $\delta^{18}O_w$ record of (*S18*) was estimated assuming a global $\delta^{18}O_w$ change of 0.5‰ per 1 salinity unit (*S22*).

Time-dependent phasing between planktonic $\delta^{18}O$ and SST

Temporal changes in the lag between planktonic $\delta^{18}O$ and SST are inferred from the location of the maximum of the cross-correlation function between the two time series. To obtain time-dependent lag estimates, the time series were analyzed within a moving window of width 40 ka. This window width offers a good compromise between statistical and systematic errors (*S23*). To facilitate the analysis, the higher-resolution $\delta^{18}O$ data were first re-sampled at the sampling times of the lower-resolution SST series. Subsequently both series were interpolated to a common sampling interval of 0.1 ka using an Akima spline (*S24*). The window was shifted consecutively by 1-ka increments along the time axis of the input time series that is close to the spacing of the original SST series.

A Monte-Carlo approach was employed to assess the uncertainty of the estimated lag values. For this purpose, 1000 lag estimates for each position of the moving window were calculated using surrogate data based on data uncertainties of 0.5°C for the SST data and 0.05‰ for the $\delta^{18}O$ data, respectively. Finally, a 95-% confidence interval was constructed from the Monte Carlo ensemble (Fig. S3).

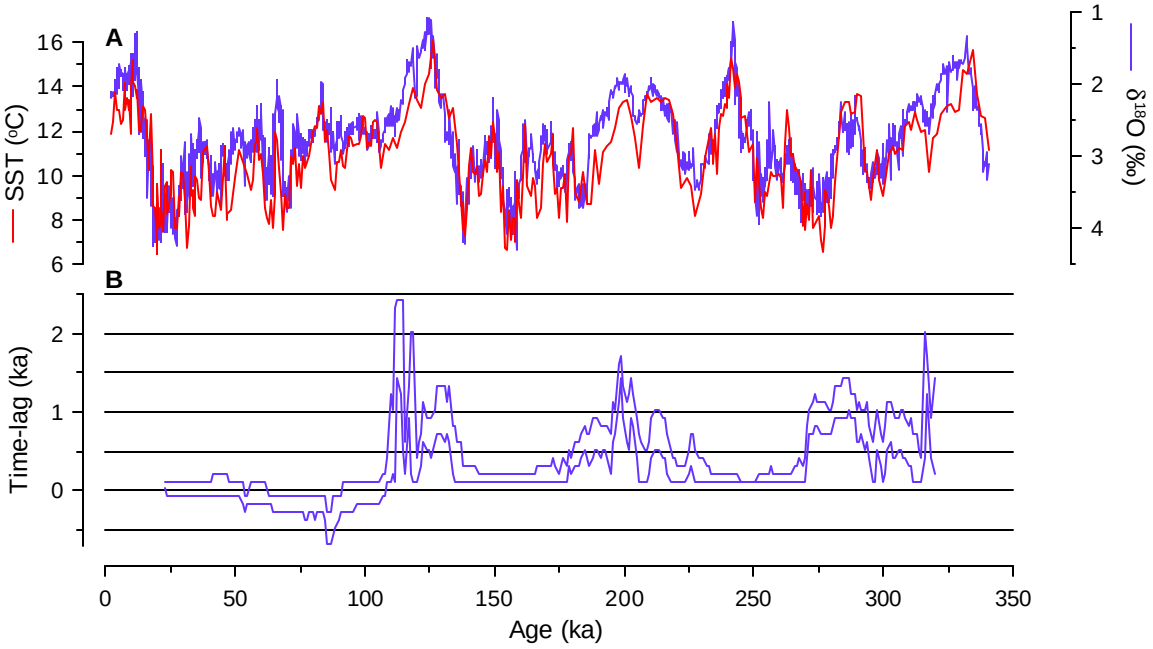

Fig. S3: (**A**) Planktonic $\delta^{18}O$ and Mg/Ca-derived SST records. (**B**) Time-dependent cross-correlation lag between resampled planktonic $\delta^{18}O$ and SST from core MD97-2120. Positive values indicate a lead of SST over $\delta^{18}O$. Shown is the 95-% confidence interval derived from the Monte Carlo simulation. Estimated lag values are plotted versus the central value of the ages within the window under consideration. Note that due to the interpolated sampling interval of the input time series, lag estimates appear as multiples of 0.1 ka.

Supporting References

S1. R. Zahn *et al.*, *Paleoceanography* **12**, 696 (1997).

S2. S. Barker, M. Greaves, H. Elderfield, *Geochem. Geophys. Geosys.* (2003 submitted).

S3. S. de Villiers, M. Greaves, H. Elderfield, *Geochem. Geophys. Geosys.* **3**, 2001GC000169 (2002).

S4. T. A. Mashiotta, D. W. Lea, H. J. Spero, *Earth Planet. Sci. Lett.* **170**, 417 (1999).

S5. H. Elderfield, G. Ganssen, *Nature* **405**, 442 (2000).

S6. J. C. Duplessy *et al.*, *Oceanol. Acta* **14**, 311 (1991).

S7. M. Stuiver, P. J. Reimer, *Radiocarbon* **35**, 215 (1993).

S8. M. Stuiver *et al.*, *Radiocarbon* **40**, 1041 (1998).

S9. A. H. L. Voelker *et al.*, *Radiocarbon* **40**, 517 (1998).

S10. C. Laj *et al.*, *Earth Planet. Sci. Lett.* **200**, 177 (2002).

S11. E. L. Sikes, C. R. Samson, T. P. Guilderson, W. R. Howard, *Nature* **405**, 555 (2000).

S12. N. J. Shackleton, M. A. Hall, E. Vincent, *Paleoceanography* **15**, 565 (2000).

S13. J. R. Petit *et al.*, *Nature* **399**, 429 (1999).

S14. N. J. Shackleton, *Science* **289**, 1897 (2000).

S15. T. Blunier, E. J. Brook, *Science* **291**, 109 (2001).

S16. C. J. N. Wilson, V. R. Switsur, A. P. Ward, *Geol. Mag.* **125**, 297 (1988).

S17. L. Carter, H. L. Neil, I. N. McCave, *Palaeogeogr. Palaeoclimatol. Palaeoecol.* **162**, 333 (2000).

S18. C. Waelbroeck *et al.*, *Quat. Sci. Rev.* **21**, 295 (2002).

S19. N. J. Shackleton, in *Les Methodes Quantitatives d'Etude des Variations du Climate au Cours du Pleistocene* L. Labeyrie, Ed. (Cent. Nat. de la Rech. Sci., Paris, 1974), vol. 219, pp. 203-210.

S20. G. A. Schmidt, G. R. Bigg, E. J. Rohling, http://www.giss.nasa.gov/data/o18data/ (1999).

S21. K. Lambeck, J. Chappell, *Science* **292**, 679 (2001).

S22. H. Craig, L. I. Gordon, in *Stable Isotopes in Oceanographic Studies and Paleotemperatures* E. Tongiorgi, Ed. (Cons. Naz. di Rech., Spoleto, 1965) pp. 9-130.

S23. M. Mudelsee, *Quat. Sci. Rev.* **20**, 583 (2001).

S24. H. Akima, *J. Assoc. Comp. Machinery* **17**, 589 (1970).